Effect of salinity diffusion and heat flux on the growth of sea ice microstructure

Yoshiki Kawano*   and   Tetsuya Ohashi**

Department of Mechanical Systems, Kitami Institute of Technology
165, Koencho, Kitami, Hokkaido 090-8507
tel. & fax.: +81-157-26-9227, e-mail: *kawa@newton.mech.kitami-it.ac.jp (corresponding author),
**ohashi@newton.mech.kitami-it.ac.jp

1. Introduction

Sea ice covers a vast area of oceans near the north and south poles and has many impacts on the environment of the earth [1)-3)]. An important effect among those is that the sea ice reflects sunlight and obstructs thermal energy to be absorbed in sea water [3)]. Therefore, the process of growth and decay of sea ice is a matter of interest.

When the sea water starts to freeze, most of salt content is discharged from ice crystals into liquid area because the solubility limit of salt in the crystal lattice of ice is very small. However, a number of small volumes of saline water, called brine regions, and air pores remain in crystal grains of ice or at grain boundaries. That is, sea ice is a porous material which is composed of pure ice crystals, brines and air inclusions. Microstructures of such ice crystals with many brine regions play a major role in the macroscopic mechanical response of ice sheet. For example, strength of sea ice is affected by brine content and its distribution in the sea ice, as well as its grain size and temperature. Assure [4)] developed pore microstructural model of sea ice and analyzed the relationship between the brine volume and macroscopic strength of sea ice. By using a Monte Carlo percolation model, Golden *et al.*[4)] showed that sea ice has a fluid permeability when volume fraction of brine regions is higher than 5 %. As stated above, physical behaviors of sea ice are closely linked to its microstructures and studies on the microstructure are very important.

Shape of ice crystals is determined by the environmental conditions under which the ice has formed [1)], and its behaviors also changes with the shape. So far, the growth process of ice crystals at molecular scale were studied by using molecular dynamics simulations [6)], and pattern formation of ice crystals were analyzed by using a discotic ice crystal model [7)]. Experimental observation of pattern formation of ice crystals in supercooled water [8)] were also made. However, behaviors of sea ice are also largely influenced by their mesoscopic structure where a lot of crystal grains and brine regions contribute. In this paper, we focus our attention at the growth process and interaction of many ice crystals and formation mechanism of brine regions at mesoscopic level.

In the previous studies [9)-12)], we developed a simple and numerically efficient simulation technique named Voronoi dynamics for the anisotropic growth of ice crystals and their impingements. Diffusion and condensation process of salinity in the seawater was also taken into account recently [12)], and it was found that Mullins-Sekerka type instability was formed at liquid-solid interface when the diffusion process governed the growth. This effect induced branching of individual crystals and resulted in a formation of lamellar shaped structure of ice platelets and brine layers. However, the effect of temperature gradient was not considered in the simulation. In this paper, heat transfer by conduction is incorporated into the model and we simulate cooling process of seawater from the sea surface.

2. Numerical procedure

2.1 Crystal growth model and solidification condition

Let us imagine the process where crystal grains grow from nuclei of crystals and impinge each other. During this process, crystal grains which have faster growth rate and earlier nucleation time occupy larger areas than others. In order to reproduce such process numerically, we use following technique, named Voronoi dynamics (Fig. 1).

(1) We assume a simulation space which is divided into small cells, and nuclei are put in the space. Each nucleus has a certain growth rate g, character number k and nucleation time. All the cells are initially given character number "-1", which means the cells are liquid (Fig.1 (a)).

(2) A time increment Δt is set so as that $\Delta t \times$ (the maximum growth rate) is less than the minimum size of the cell.

(3) Then, we advance the time from t to $t+\Delta t$, and check if growths from nuclei reach to each cell. If growth of a nucleus with the character number k reaches to a cell, and if the cell is touching to a cell that was already solidified and have character number k, the character number of the cell is changed from -1 to k, which means the cell is solidified (Fig.1 (b)).

(4) The procedure (3) is repeated with a time interval Δt and solidification of cells progresses. After a certain time increments, aggregates of solidified cells with the same character number are formed and each of them are individual crystal grains (Fig.1 (c)).

In the above procedure, crystal structures are built up as a result of scrambles for the area (cells) by the nuclei, and only the geometrical effect by the mutual impingement of growth of the crystallites is considered. However, when ice crystals grow in sea water, salt content in sea water is discharged from ice crystals into solid-liquid interface during crystal growth, and the salinity is condensed at the interface and such high salinity impedes the growth of crystals. To reproduce this effect, we incorporate the following model into the Voronoi dynamics scheme.

When a liquid cell solidifies, salt content in the cell is discharged to its neighboring cells. Fig.3 schematically illustrates the movement of salt content from a newly solidified cell. We assume that the salt is equally distributed from the newly solidified cell to its neighboring non-solidified cell(s).

Relationship between salinity S_b and solidification temperature T_s of sea water is approximately given by a monotonically decreasing function of S_b [2]:

$$T_s = \frac{54.11 S_b}{S_b - 1000} + 273.15 \quad \left(250.15 \leq T_s \leq 273.15\right) . \tag{1}$$

Liquid cells can solidify when the temperature is lower than the solidification point, and this condition is added to the solidification condition of Voronoi dynamics.
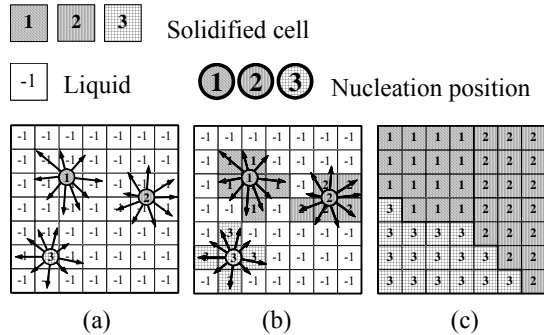

Fig. 1   Schematic illustration of Voronoi dynamics technique.
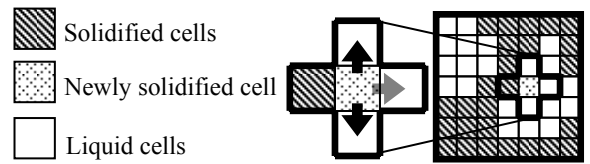

Fig. 2   Discharge of salinity from newly solidified cell. All the discharged salinity is distributed equally to neighboring liquid cells.

2.2 Salinity diffusion and conduction of heat

Diffusion of salinity is expressed by Fick's second low:

$$\frac{\partial C_{salt}}{\partial t} = D \left(\frac{\partial^2 C_{salt}}{\partial x^2} + \frac{\partial^2 C_{salt}}{\partial y^2} \right), \tag{2}$$

where C_{salt} and D denote density and diffusion coefficient of salt, respectively. Salinity diffusion process occurs only between liquid cells. Temperature T changes by conduction of heat and the

temperature distribution is governed by the following equation:

$$\frac{\partial T}{\partial t} = a\left(\frac{\partial^2 T}{\partial x^2} + \frac{\partial^2 T}{\partial y^2}\right),$$

(3)

where a is the thermal diffusivity. Physical constants for seawater or pure ice are used in each of the cells in accordance with their liquid or solid state. Eqs. (2) and (3) are discretized by using the same space grid as the one used for the Voronoi dynamics and solved by finite difference method with forward Euler's time integration scheme.

2.3 Growth rate model of nuclei

Generally, ice crystals have a six-fold symmetricity in the basal plane and growth rate is not isotropic. For the expression of such anisotropic growth characteristics, we assume that c-axis of nuclei is normal to the simulation space and the growth rate g in the basal plane is expressed by a simple equation given by:

$$g^{(k)}(\theta) = g_0 + g_{ax} \times \cos\left(n_s\theta + \alpha^{(k)}\right),$$

(4)

where, g_0 denotes the average growth rate, g_{ax} gives the magnitude of deviation from the average, and integer number n_s(=6) defines the number of symmetricity, and θ is the direction of growth. α, which is given by a random number between 0 and 2π, defines the orientation of crystallites (Fig. 3).
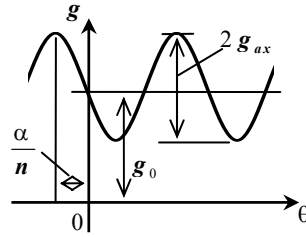

Fig. 3   Anisotropic growth rate given by eq. (4).

3. Results and discussion

Let us assume a homogeneous sea water area for the simulation space. Dimension of the space is 50×150mm^2 and the space stands vertically. The upper edge of the space coincides to the sea surface and the space is filled with sea water with salinity 35 ‰. 30 points are randomly chosen near the upper edge of the simulation space as the candidate position for nucleation of crystallites. The nucleation is supposed to takes place when the temperature at the candidate position becomes lower than the solidification temperature T_s. Physical constants of ice and seawater used in the both simulations are shown in Table.1. Two simulations are performed with different conditions for temperature and growth rate of crystals.

In the first simulation, we assume that g_0=0.00106mm/s, $R_{anisotropy}$=0.3 and n_s=6. The whole simulation space is kept at -4℃ during crystal growth. Obtained results are shown in Fig. 4.

In the second simulation, g_0=0.1 mm/s and initial temperature in the whole simulation space is -1℃. Then, the sea surface is cooled and kept at -5℃, while the bottom of the space is kept at -1℃. In this condition, temperature gradient is developed in the specimen with progress of time. Obtained results are shown in Fig. 5.

Figs.4 (a)-(e) and Fig.5 (l) show salinity distributions and Figs.5 (a)-(e) depict distributions of degree of supercooling σ[%] which is defined by

Table. 1   Physical constants used in the present simulations.

	Ice	Seawater
Diffusion coefficient of salt D [m^2/s]		6.8×10^{-10} [13]
Specific heat c[J/kgK]	2040	4217
Diffusivity of heat a[m^2/s]	1.17×10^{-6} [14]	0.139×10^{-6} [15]
Density ρ[kg/m^3]	916.8	1000

$$\sigma = \frac{T_s - T}{T_s} \times 100 .\tag{8}$$

In these figures, white regions show crystals. Fig.4 (f) and Fig.5 (f) show crystal structure at t=5000s, where individual grains are identified by different gray colors. Figs.5 (g)-(k) show change of temperature distribution with time. Fig. 5 (l) is the salinity distribution at t=5000s.

Fig. 4 shows the results of the first simulation where temperature is maintained uniform and constant throughout the simulation schedule. In the initial stage of crystal growth (Fig.4(a), (b)), the crystallites grow mostly independently in stellar shape. Salt is discharged from solidified area to their environments and high salinity layers build up around them. Degree of supercooling near the ice-seawater interface is small due to the high salinity layers and crystal growth becomes to be governed by salinity diffusion process. Once this condition is formed, solidification progresses more at protrudent place where diffusion of salinity is quicker. The protrusion is amplified with time and the growth is unstable. As a result, the solid-liquid interfaces which are initially smooth become to be rough and areas of condensed seawater are formed at small concave regions between protruded solid regions.

In the concave region, space for diffusion is limited and its salinity is not easily lowered. Thus, the condensed sea water in the concave regions become to be difficult to solidify, and the regions turn out to be non-solidified regions within the grains. This phenomenon is observed not only in the early stages of crystal growth where granular shaped grains are formed near the surface but also in the stages where columnar shaped grains are formed at lower part of the sea ice (Fig.4 (c)-(e)).

(a)t=50s   (b)t=200s   (c)t=400s   (d)t=1000s   (e)t=5000s   (f)t=5000s
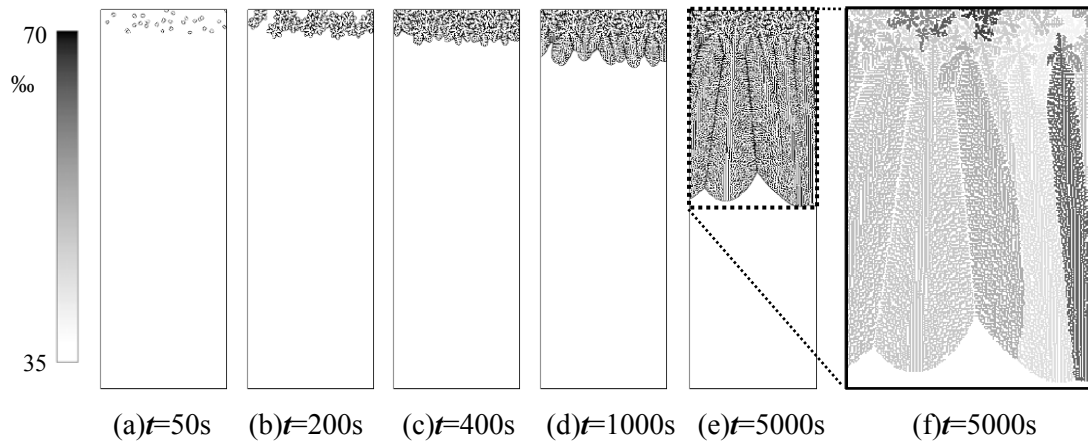
Fig.4   Obtained results when temperature gradient does not exist.   (a)-(e) are salinity distributions and (f) shows crystal structure.

Next, we observe the result of the simulation with considering the effect of temperature gradient (Fig. 5). In the early stages of the crystal growth (Fig.5(a)), where ice crystals has not completely covered the sea surface, a layer of high degrees of supercooling build up near the sea surface. Thus, growth rates of the crystals become faster in horizontal direction than in downward direction, and the growth mainly develops near the surface (Fig.5 (b)). Since the diffusivity of heat is higher in the ice crystal than that in the seawater, then the temperature in and around the crystal becomes lower (Fig.5 (g), (h)). Once the surface is covered by the sea ice and the thickness of the sea ice increases (Figs. 5 (i), (j)), temperature distribution in the horizontal direction becomes more uniform. After that, fluctuation of temperature in the horizontal direction is kept very small and temperature at deeper level decreases with time (Fig.5 (k)).

Growth of ice crystals at solid-liquid interface becomes unstable by the effect of high salinity layers, which is similar to the case shown in Fig.4, and condensed seawater is trapped within the ice crystals in the granular zone. However, in the zone of columnar crystals, formation process of brine regions differs from that obtained in the first simulation. In the zone of columnar shaped grains of Fig. 5, growth rate of most grains in the

downward direction becomes almost the same due to the effect of uniform temperature in the horizontal direction. Then, growth rates of thin ice arms protruded from irregularities at interface also become almost the same and growth directions also align. Areas of condensed sea water are left behind between the protrusions, and the tips of the protrusions keep advancing in the downward direction without connecting each other due to the condensed seawater between them and high temperature around the tips (Fig.5 (d)). As a result, in the columnar zone ice, lamellar-like structure which consists of brine layers and thin ice plates are formed in the vertical direction (Fig. 5 (e), (f)).

Fig.5 (l) shows the distribution of salinity at t=5000 s. We find that salinity near the sea surface is higher. This is because the temperature is lower near the sea surface (Fig.5 (k)) and solidification is easier. As a result, areas of brine regions near the sea surface become smaller than those in the lower part of the sea ice.
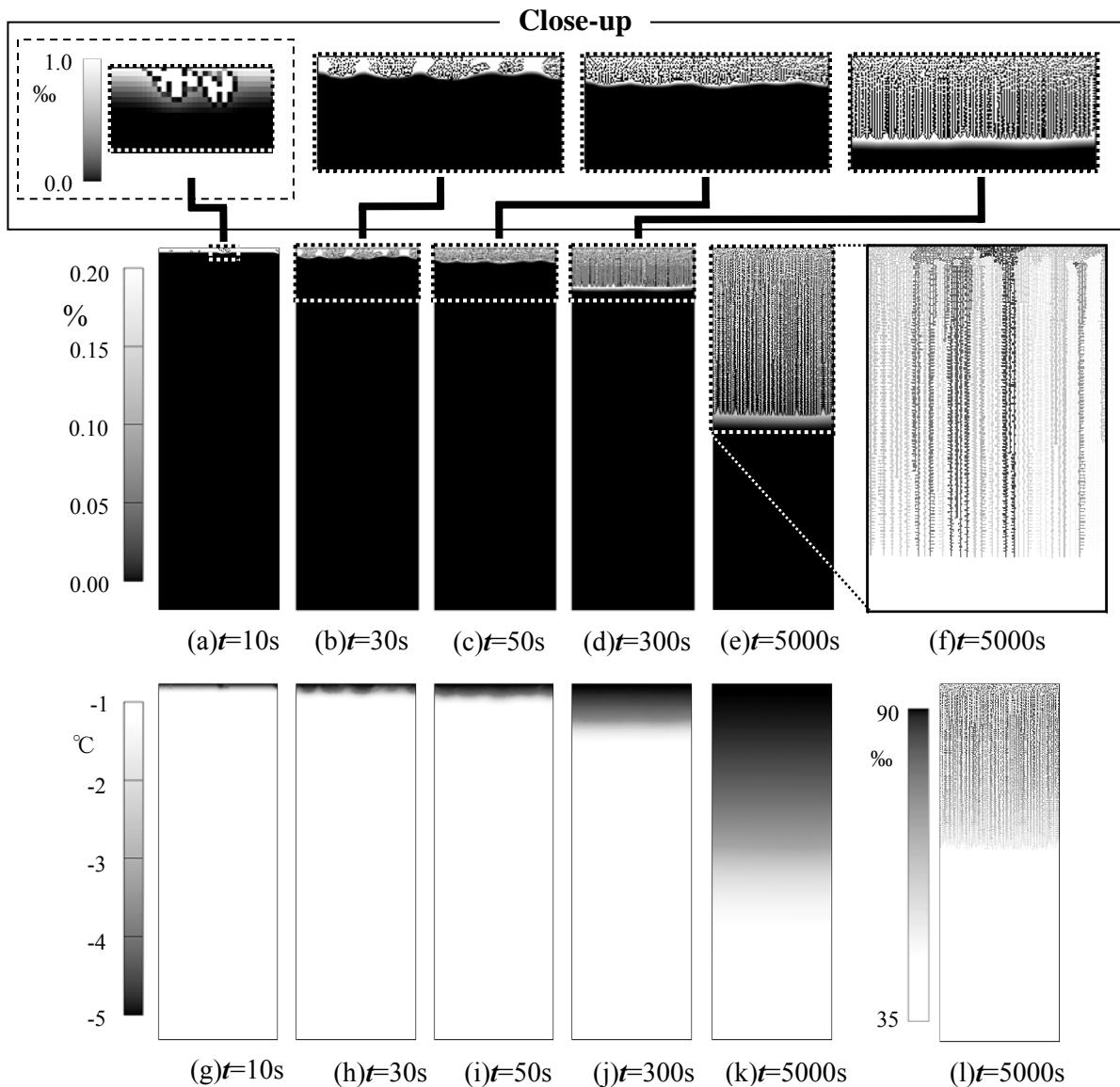

Fig.5 Obtained results when temperature gradient exists in the specimen. (a)-(e) are distributions of degrees of supercooling of seawater, (f) is crystal structure, (g)-(k) are temperature distributions and (l) shows salinity distribution.

4. Conclusion

In this paper, we numerically simulated the growth process of sea ice polycrystals by using models for crystal growth, salinity diffusion and heat conduction.   Obtained results are summarized as follows.

1. By the effect of temperature gradient, fine branching arms of growing crystals aligned in vertical direction, and they formed lamellar like structure.
2. By the effect of temperature gradient, sizes of brine regions became smaller near sea surface than those at deep place of the sea ice.
3. By the effect of temperature gradient, salinity in the brines at shallower place in the sea ice crystal was higher than those at deeper place.

References

1) Weeks, W.F. and Ackley, S.F., The growth, structure and properties of sea ice, *CRREL Monograph*, (1982).
2) Eicken, H., Growth, Microstructure and Properties of Sea Ice, In: Thomas, D.N., Dieckmann, G.S. (Eds.), *Sea Ice: An Introduction to its Physics, Chemistry, Biology and Geology. Blackwell, Oxford*, (2003), pp. 22-81.
3) Wakatuchi, M., freezing sea (Koru Umi), In: Hukuda, M., Akira, K., Takahashi, S. (Eds.), *Science in polar region* (*Kyokuti no Kagaku*), pp. 15-26
4) Assur, A,. Composition of sea ice and its tensile strength, *Proceedings of the Arctic Sea Ice Conference, Easton*, (1958), pp106-138.
5) Golden, K.M. Ackley, S.F., Lytle, V.I., The Percolation Phase Transition in Sea Ice, *SIENCE*, Vol. 282, (1998), pp. 2238-2241.
6) Noda, H., Von der Eerden, J. P., Furukawa, Y., A clear observation of crystal growth of ice from water in a molecular dynamics simulation with a six-site potential model of H_2O, *Journal of Crystal Growth*, Vol. 266, (2004), pp. 297-302.
7) Yokoyama, E., Sekerka, R.F., Growth trajectories of disk crystals of ice growing from supercooled water, *J. Phys. Chem. B*, Vol. 104, (2000), pp. 65-67.
8) Shimada, W., Furukawa, Y., Pattern formation of ice crystals during free growth in super cooled water, *J. Phys. Chem. B*, Vol. 101, (1997), pp. 6171-6173.
9) Ohashi, T., Sasaki, M., Yoshimura, Y., *Proc. 19th int. symp. on Okhotsk sea & sea ice*, (2004), pp. 180-185.
10) Kawano, Y., Ohashi, T., Numerical simulation for development of polycrystal microstructure of sea ice and brine formation by salinity concentration, *Proc 21th int. symp. on Okhotsk sea & sea ice*, (2006), pp. 95-.98
11) Kawano, Y., Ohashi, T., Numerical simulation of development of sea ice microstructure by Voronoi dynamics technique, *Proc. 18th IAHR Int. Symp. on Ice*, Vol. 2 (2006), pp. 97-103
12) Ohashi, T., Kawano, Y., Numerical simulation of salinity diffusion and growth instability in the microstructure evolution of sea ice, *Proc. 22th int. symp. on Okhotsk sea & sea ice*, (2007), pp. 11-16
13) Yoshiaki, T., Kaimen kyokai katei, In: *Physical oceanography* (*Kaiyo butsuri*), *Tokai univ. press*, Tokyo, pp. 145-263.
14) Okagaki, O., Conduction of heat (Netsu Dendo), In: Nobuhiro S. (Ed.), *Engineering of heat transmission* (Dennetsu Kogaku), (1998), *Morikita press*, p.5.
15) The Japan Society of Mechanical Engineers ed., *Data book of Engineering of Heat Transmission* (*Dennetsu Kogaku Shiryo*), (2003), p.353, The Japan Society of Mechanical Engineers.